Effect of coil charge duration on combustion variability and flame morphology in a GDI engine working in lean burn conditions

Effect of coil charge duration on combustion variability and flame morphology in a GDI engine working in lean burn conditions

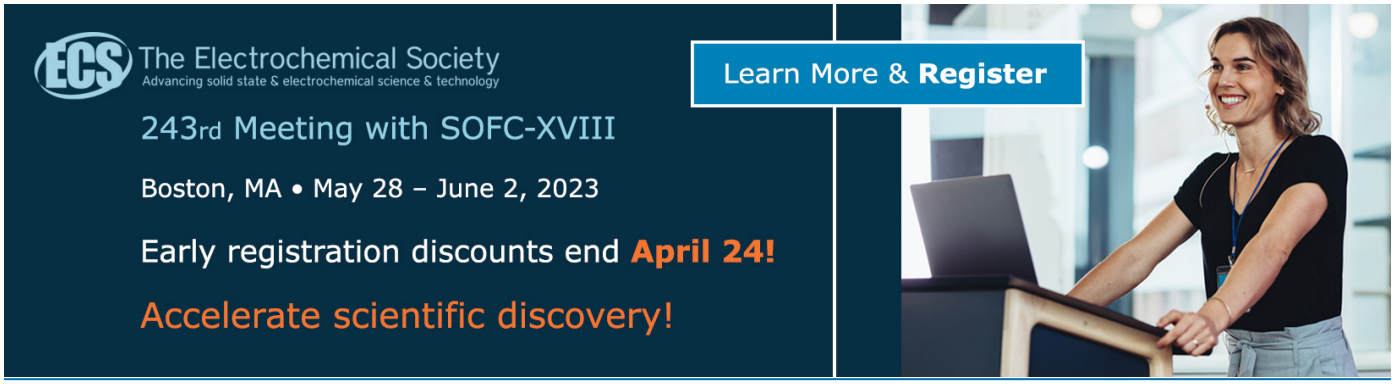

Effect of coil charge duration on combustion variability and flame morphology in a GDI engine working in lean burn conditions

G Cecere[1,2], S S Merola[1], A Irimescu[1], F Millo[2], L Rolando[2]

[1] CNR STEMS_ Science and Technology Institute for Sustainable Energy and Mobility, 80125 Napoli, Italy;
[2] Politecnico di Torino, 10129 Torino, Italy

[1] giovanni.cecere@stems.cnr.it;adrian.irimescu@stems.cnr.it; simonasilvia.merola@stems.cnr.it
[2] federico.millo@polito.it; luciano.rolando@polito.it

Abstract. Spark ignition (SI) and subsequent flame front development exert a significant influence on cyclic variability of internal combustion engines (ICEs). The increasing exploitation of lean air-fuel mixtures in SI engines to lower fuel consumption and CO_2 emissions is driving the scientific community towards the search for innovative combustion strategies. Moreover, although lean combustion has been widely investigated and an important number of studies is already present in literature, the high cyclic variability typical of this combustion process still represents a major hinder to its exploitation. This study aims to investigate the effects of increasing ignition energy on combustion characteristics of lean mixtures. Tests were performed on an optically accessible gasoline direct injection (GDI) engine that allowed to investigate the correlation between the thermodynamic results and spark arc-flame morphology. Engine speed was fixed at 2000 rpm, a relative air fuel ratio (AFR_{rel}) of about 1.3 was selected and ignition timing was set at 12 crank angle degrees (CAD) bTDC. Coil charge duration was swept from 10 to 40 CAD. Two intake pressure levels were investigated, the first corresponding to wide open throttle under naturally aspirated operating mode, the second with an intake pressure of 1.2 bar, thus corresponding to a boosted operating condition. Two dedicated scripts built using NI Vision were employed for image processing, allowing the evaluation of temporal and spatial evolution of the early stages of combustion. Arc elongation and flame front contour were used as correlation parameters that characterize flame kernel inception and development. The results confirm that, as expected, the increase of the coil charge duration tends to reduce cyclic variability in terms of engine output. The optical investigations revealed that for both examined cases the standard deviation related to the wrinkling effect on flame edge at CA5 decreased as the coil charge duration increased.

1. Introduction

Despite the latest announcement of the European community which confirmed its willingness to join fit for 55 plan [1] to achieve the net zero CO_2 emissions by 2050, the internal combustion engine is expected to play a key role in the road transport sector for the next decades [2], both as main component (i.e., in a single power source architecture) and included in a hybrid architecture [3]. The IC engines, more precisely spark ignition engines, have been subjected to many studies and

improvements for more than a century; Downsizing usually associated with turbocharging[4], the use of recirculated exhaust gas (EGR) [5], alternative injection layout/strategies [6], represent only some of the main techniques or combustion strategies that have been used for enhancing the IC engines efficiency in the last decades. Also, in order to reduce the fuel consumption and CO_2 emissions, the use of lean burn strategies is gaining a renewed interest from the scientific community. Representative of the latter is the PHOENICE project [7] funded by the EU which aims at developing a plug-in hybrid C-SUV vehicle that can demonstrate the reduction of the fuel consumption and pollutant emissions for real world driving conditions by coupling the use of alternative fuels and high diluted air-fuel ratio. Nevertheless, further margins of improvement are still available, and the stricter greenhouse gas emissions (GHG) levels required year after year to tackle the climate crisis are driving towards their research. Then, this study focuses its attention on the early stages of the combustion process, more in detail in a range that moves from the spark arc inception up to the flame front at the instant corresponding to the ten percent of burned fuel mass fraction (MFB). This phase is pointed to play a key role for the generation of the Cycle-to-Cycle Variability (CCV). Furthermore, several studies were conducted to gain a deep understanding of the phenomena underlying the CCV; Pera et al in [8] performed a 2D direct numerical simulations (DNSs) coupled with semi-detailed chemistry solving model for isooctane in the early flame kernel growth to investigate how turbulence influence combustion variability generation. Their main findings suggested the initial flame kernel dimension represented the main contributor to combustion variations and its relevance grow employing lean mixtures. Moreover, Aleiferis et al in [9] investigated the OH and CH radical intensifies in an optically accessible stratified engine to evaluate the global and local equivalence ratio of the reacting mixture and its contribution to the flame growth and cyclic variability. The resultant OH and CH production curves obtained by the variation of the global air-fuel ratio (AFR) highlighted an opposite behaviour of the two radicals, furthermore, it was noted a high cyclic variability of the local reacting mixture around the spark plug. Given the high sensitivity of the CCV to the mixture composition demonstrated by several studies, many researchers focused their attention on injection strategies. For instance, Duan et al in [10] examined how various injection strategies affected the combustion process and more in detail how them influenced the generation of cyclic variability. The authors of the above work employed two main strategies, the first based on a single injection event, while for the second the injection was split in two events. Hence, it was noted that the Coefficient of Variations (COV) of the main combustion parameters (i.e., pressure peaks, indicated mean effective pressure IMEP, combustion duration CA10-90, and so on..) strongly decreased as employing the two injection strategy thanks to the enhanced air-fuel mixing. In [11] the authors performed an investigation on the same experimental set up used for the current work combining the thermodynamic and optical analysis to correlate the combustion variability with the main morphologic parameters of the flame kernel. One of the main findings was linked to the upper and lower limit of kernel diameter size which was found to be an indicator of the cyclic dispersion. After the above considerations, in a context where increasingly leaner mixtures are employed for SI engines, the present work contributes to provide detailed insight about the coil charge duration influence on first stages of the combustion process for two operating conditions, i.e., Wide Open Throttle (WOT) and boosted. In the current study, experimental tests were performed in an optically accessible engine working in lean burn condition by coupling thermodynamic and optical analysis. The coil charge duration was swept as to almost reach the flammability limits of the reacting mixture. As concerns the optical analysis, the main morphologic parameters of the arc and flame at CA5 were examined by using two ad-hoc image processing techniques that offered the possibility to extent the overview of fundamental research results on the interaction between ignition strategies and first phase of combustion process.

2. Experimental setup

Measurements were performed on an optically accessible Direct Injection Spark Ignition (DISI) engine which was suitably modified from a commercial 1.4 litres, four valves per cylinder, 4-cylinder in line engine. The optical access to the combustion chamber was created using a Bowditch extended piston design. Table 1 lists the main engine specifications. Figure 1A shows an overview of the experimental setup comprehensive of the high-speed camera position with respect to the engine, while

Figure 1B a detailed sketch of the in-cylinder top section is presented in order to highlight the spark plug orientation and coordinate reference system used for the following considerations.

Table 1. Engine specifications

Parameter	Description
Displacement	399.0 cm^3
Stroke	81.3 mm
Bore	79.0 mm
Connecting Rod	143.0 mm
Compression Ratio	10:1
Number of Valves	4
Exhaust Valves Opening	153 CAD ATDC
Exhaust Valves Closing	360 CAD ATDC
Intake Valves Opening	363 CAD BTDC
Intake Valves Closing	144 CAD BTDC
Fuel Injection System	DI WG
Start of Injection	300 CAD BTDC

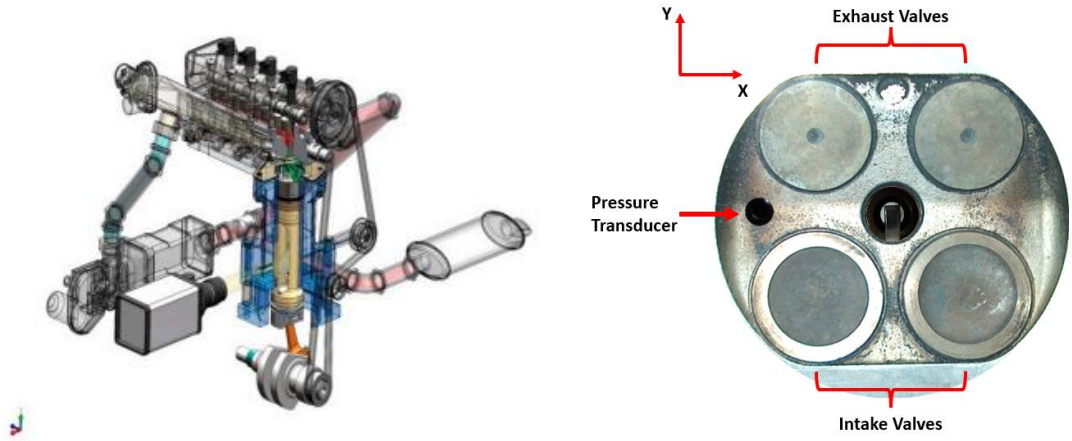

A B

Figure 1. (**A**) Experimental set-up overview, (**B**) combustion chamber view by the optical access.

The spark plug chosen for this work is a single J-Type design (Bosch YR7LEU) with a fixed uni-flow orientation in which the ground electrode is parallel to the tumble motion which is predominant along the Y axis (Figure 1B). For each test, 200 consecutive in-cylinder pressure cycles were recorded using a piezo-electric transducer (AVL GH12D) with an accuracy of ±1% and crank angle resolution of 0.2 CAD, then using a dedicated script built on NI LabVIEW 2019 environment it was possible to obtain a single mean pressure signal. For the intake air conditions, the temperature was controlled by using a thermocouple placed in the manifold and the pressure measured by a piezo-resistive sensor. The DI system featured a Wall Guided (WG) configuration and the relative A/F ratio was monitored with a Universal Exhaust Gas Oxygen (UEGO) sensor. In Table 2 are listed the engine operative conditions examined.

Table 2. Operative conditions

Engine Speed [rpm]	Spark plug design	Orientation	Intake pressure [bar]	Spark advance [CAD BTDC]	λ	Coil Charge Duration [CAD]
2000	J - Type	Uni-flow	0.98	12	1.30	10 - 20 - 40

1.20	-	-	-

3. Optical setup and methodology

The early stages of the combustion process were acquired by using a high-speed CMOS camera (CamRecord 5000, 8-bit, 16 μm x 16 μm pixel size by Optronis, Kehl, Germany) equipped with a 50 mm focus Nikon lens. The camera worked in full chip configuration and the acquisition rate was set at 5000 frames per second with an exposure time of 167 μm. In order to improve the singal-noise ratio, the f-stop (i.e., ratio between the focal length of a lens and the diameter of the diaphragm into which light enters) of the lens was set at 2.8. The set-up allowed to record the images with a dwell time of 2.4 CAD at 2000 rpm and a spatial resolution of about 0.19 mm per pixel. The optical acquisition for each operative condition consisted of 25 frames per cycle starting from the spark ignition. Two distincts scripts were built in NI Vision 2020 enviroment as to achieve quantitative information by the arc and flame front at CA5 and CA10 respectively. The fundamental steps of the image processing procedure were the same for both scripts and are showed in Figure 2.

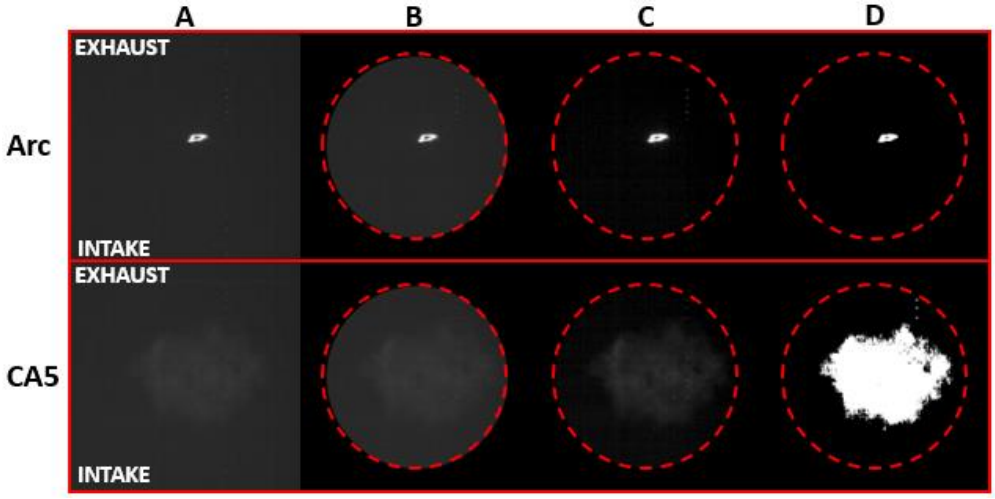

Figure 2. (**A**) Raw image, (**B**) Circular mask application, (**C**) image improvement, (**D**) image binarization. Operative case; P_{IN} 1.2 bar, Coil charge duration 40 CAD.

Starting by the raw images, a circular mask was applied to all 256-grey scale image sequencies as to identify the optical window limits and cut off the light reflections coming from the in-cylinder boundaries. Then, the gamma, contrast and brightness levels were adjusted for highlighting the arc/flame with respect to the background. The values adopted in this phase were 128, 53.30 and 1.00, for brightness, contrast, and gamma respectively. The next step involved the binarization of the so obtained optimized image through the choice of a suitable threshold level. Considering the different luminosity intensity reached by the arcs and flames at CA5 and CA10, the threshold level was set at 128/256 for the first and varied in a range between 22-25/256-grey scale for the fully developed flame. At this point, given the small size of the arc compared to the entire investigated area, only the flame front binarized images were corrected using advanced morphology tools in order to remove any small objects not included in the flame front or for filling any holes. In fact, the use of filtering functions on frames corresponding to the arc inception instant could clearly influence their morphological parameters, then altering and invalidating the subsequent considerations. The last phase of the image processing procedure expected the use of feature detection function. This latter uses an algorithm to find the geometrical coordinates of the points along the object contour with a certain accuracy set by the user. The feature detection function had two well defined purposes for the current work; for the frames relative to the arc, it was used to characterize the maximum elongation, while for the flame at

CA5 and CA10 on the contour distribution (i.e., wrinkling effect of the flame front and relative centre dislocation with respect to the spark plug). Furthermore, the flame front edge distribution was calculated both with respect to the geometrical centre (i.e., corresponding to the mass electrode spark plug centre) and flame mass centre (i.e., defined as the arithmetical centre of the binarized flame image) to separately study the weight of dislocation and wrinkling effect on global distortion. Then, by calculating the distance R between the so chosen referment centre and edge points with the following equation (1),

$$R_i = \sqrt{(X_i^2 + Y_i^2)} \quad (1)$$

it was possible to extrapolate the flame contour statistical distribution. The Figure 3 shows how the edge detection functions worked for each case.

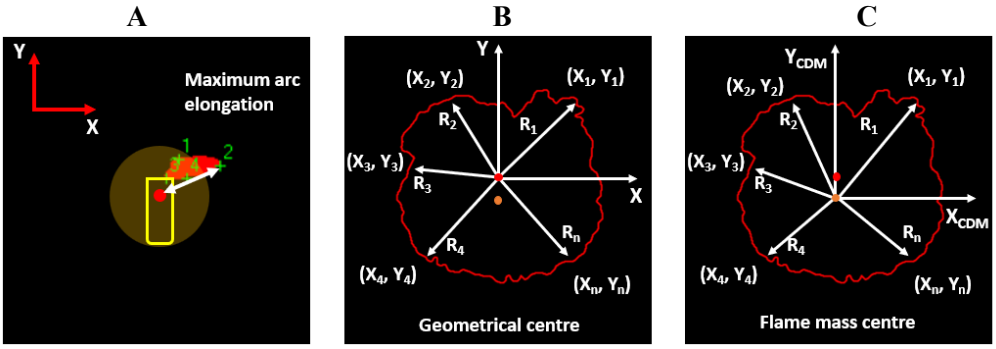

Figure 3. (**A**) Maximum arc elongation, (**B**) flame contour distribution with respect to the geometrical centre (red circle), therefore taking into account both dislocation and wrinkling effect, (**C**) flame contour distribution with respect to the flame mass centre (orange circle), only wrinkling effect.

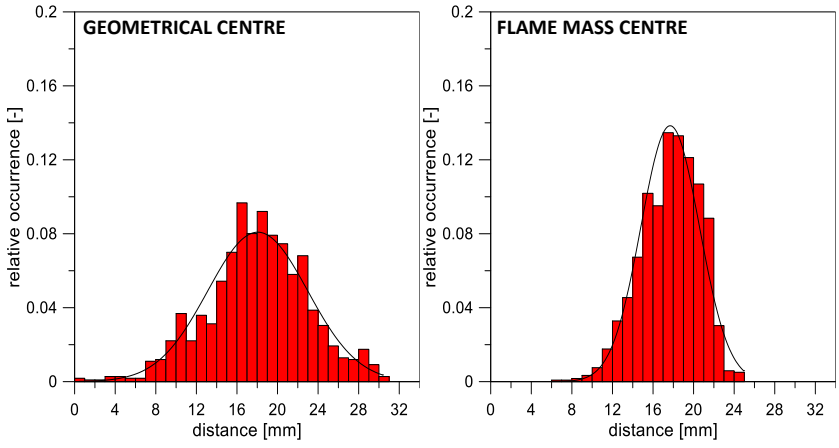

Figure 4. Flame contour distribution with respect to the geometrical centre (**left**) and flame mass centre (**right**). Operative case; Wide open throttle condition, coil charge duration of 40 CAD.

Figure 4 shows two contour distributions highlighting how the dislocation effect plays an important role in the global distortion of the flame.

4. Results

The results of the current work are organized with an increasing level of detail, starting by an overall overview of the combustion process parameters, and then moving to a more detailed discussion on the findings of the optical investigation performed on the early stages of combustion process.

4.1. Thermodynamic results

In Figure 5 an overview of the combustion process performance can be inferred with the average signals of in-cylinder pressure (top), indicated mean effective pressure (IMEP, bottom) values and its coefficient of variation (COV, bottom). As expected, considering that all the data treated in this section derive from an average on 200 cycles, the boosted operative condition featured higher in-cylinder pressure (i.e., pressure peak) and IMEP, while the overall level of COV resulted much more contained with respect to the wide open throttle (WOT) case. More in particular, the coil charge duration appears to affect only in minor way the in-cylinder pressure and IMEP, with the only slight variation recorded for the average pressure traces relative to the turbocharged condition (i.e., close to the pressure peak location it was noted a maximum gap of about 1.2 bar between the cases with a coil charge duration of 10 and 20 CAD) but without any reflection on the IMEP level. On the other hand, for both operative conditions, the combustion stability, strongly related to the COV_{IMEP}, appeared to be clearly influenced by the increase of the coil charge duration. More in detail, an absolute decrease of 1.5% for the WOT condition and of 0.4% for the turbocharged was noted passing from 11.8% to 10.3% and 5.0% to 4.6% respectively. Regarding the heat release rate, it is not present in this work as the latter did not add any relevant information about the combustion process (i.e., the NHRR profiles were close to each other without highlighting any substantial differences).

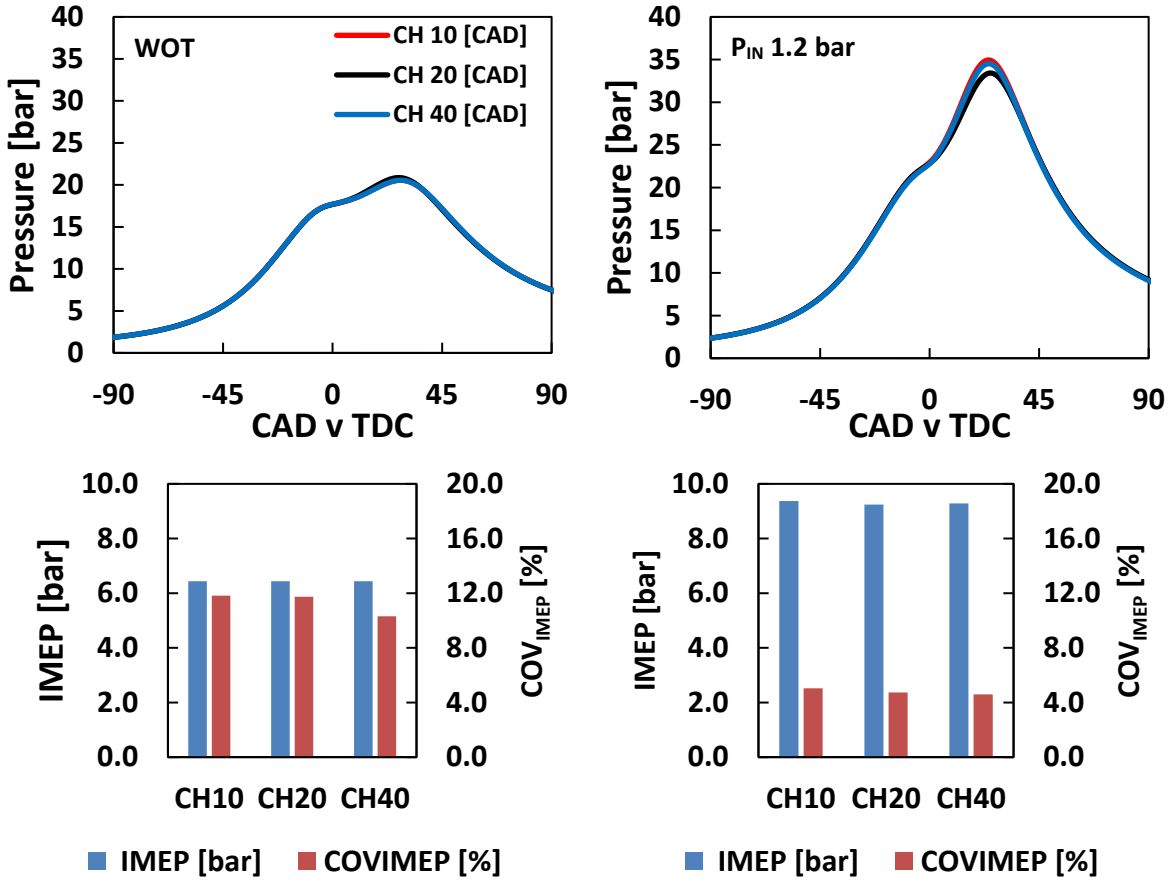

Figure 5. (**top left**) Wide open throttle in-cylinder pressure traces, (**top right**) boosted pressure traces. (**bottom left**) Indicated mean effective pressure and its COV for WOT condition and (**bottom right**) boosted one.

Optical results

Main areas of interest of the optical analysis were the spark arc and flame front distribution at CA5 and CA10. Therefore, in Figure 6 the maximum arc elongation and its Feret diameter (i.e., the

maximum distance between two parallel planes containing the investigated object) are presented for each case examined.

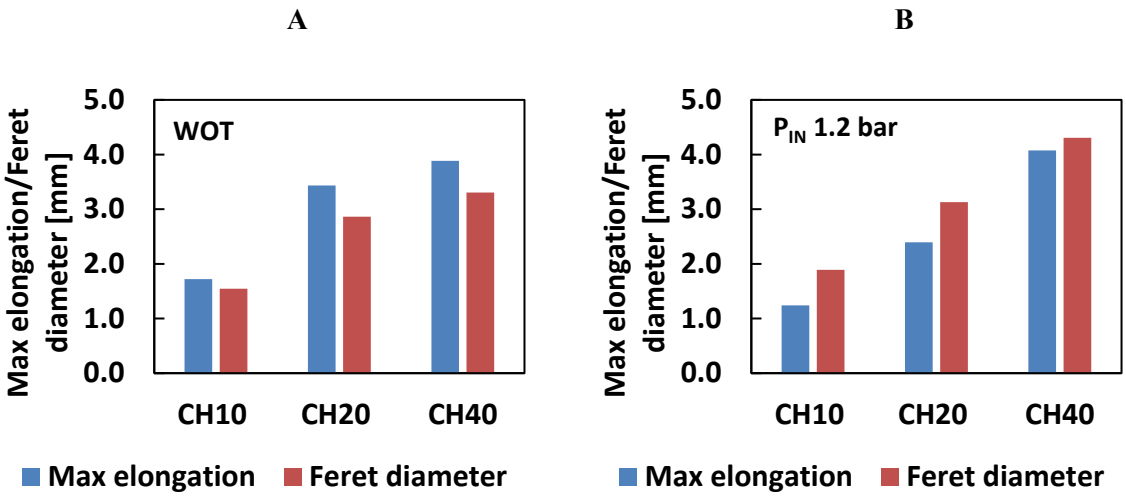

Figure 6. (**A**) Maximum arc elongation and arc Feret diameter for WOT condition and (**B**) boosted one.

As expected, giving more energy to the spark ignition resulted in an increased arc elongation with respect to the geometrical centre and size for both operative conditions investigated. Looking at the Feret diameter, it appears that the WOT case was able to ensure higher size of arc for reduced coil charge duration, while the turbocharged condition for the most extended. Then, reminding the above Figure 5, the COV reduction for both cases (bottom figures, red bars) resulted in an increased arc elongation that allowed to have a more stable kernel inception process, with subsequent improved combustion stability. In Figure 7 a representative sequence of flame edge distributions at CA5 and CA10 is shown. The images were chosen to illustrate and highlight the different weight that dislocation and wrinkling effect have on the flame propagating process.

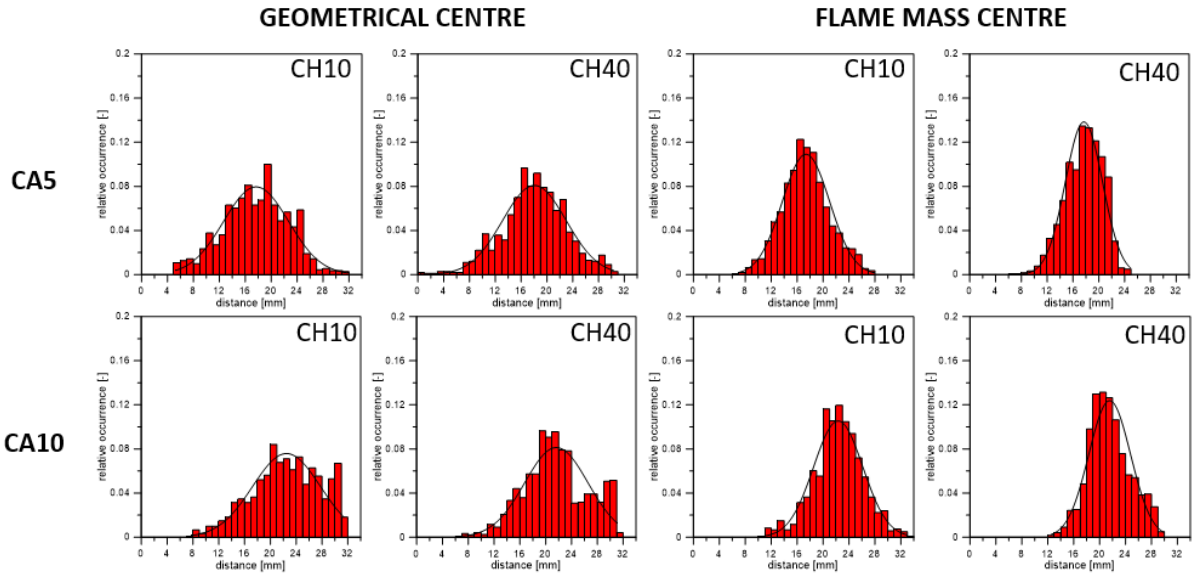

Figure 7. Flame front edge distribution with respect to the geometrical (**left**) and flame mass centre (**right**). Operative case; Wide open throttle condition, coil charge duration of 40 CAD.

As expected, looking at Figure 7, when considering only the wrinkling effect (Figure 3), the amplitude of distribution decreases (i.e., practically the standard deviation). Furthermore, observing the histograms relative to the flame mass centre, the distributions suggest that globally the flame contour at CA5 and CA10 tends to remain quite "circular" without any relevant distortion. In order to have a clearer idea about the above behavior, Figure 8 shows the standard deviation (σ) values of the gaussian curves that best matched the experimental distributions of the flame front.

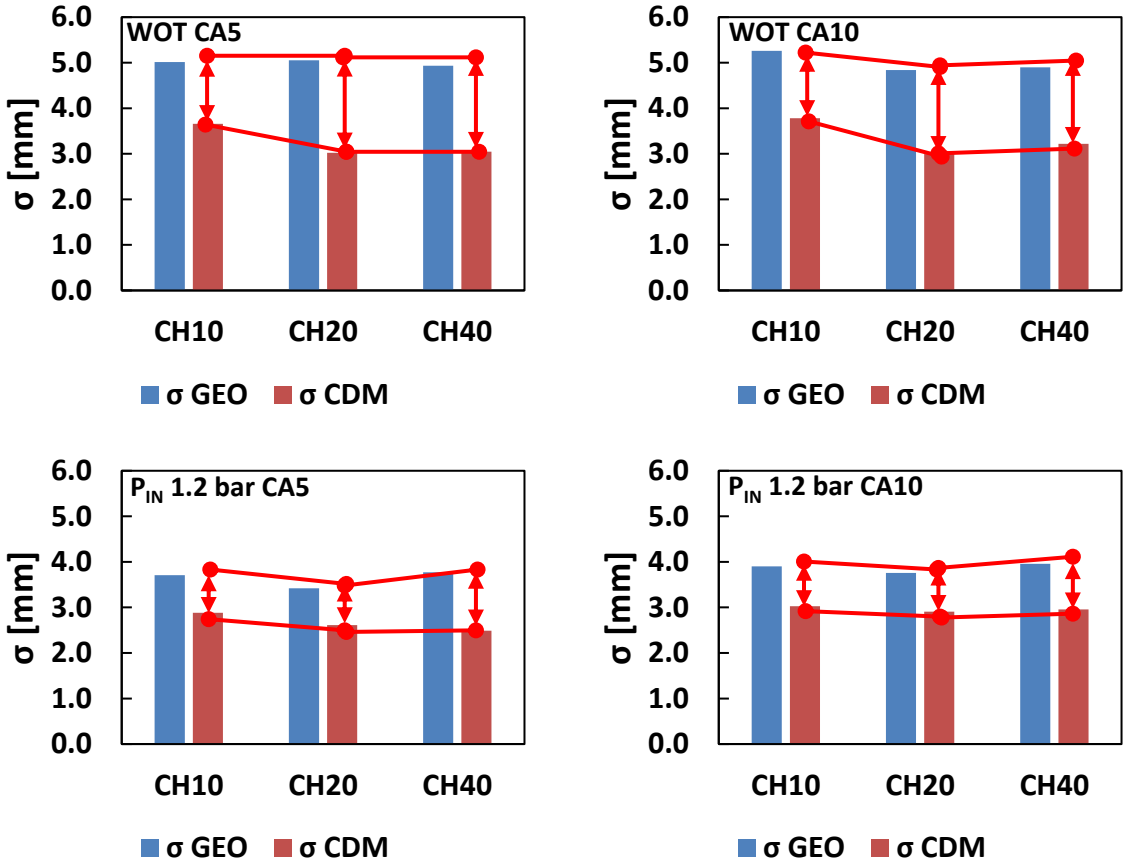

Figure 8. Standard deviation values of flame front radius at instant corresponding to the CA5 (**left**) and CA10 (**right**). Operative cases; Wide open throttle (**top**) and P_{IN} 1.2 bar (**bottom**).

By Figure 8 it is possible to observe how the increase of energy given to the arc influences the flame front wrinkling effect reducing it, P_{IN} 1.2 bar - CA10 excluded. For both cases, this influence results more evident when passing from CH10 to CH20, then remaining on similar values or slightly lower when passing to the CH40 operative point. More in particular, for the WOT condition σ recorded a relatively decreases by about 20% for both instants at CA5 and CA10. For the boosted case, the relative reduction at CA5 is slightly less than 12%. The weight of the dislocation of the flame mass centre, which is roughly conceivable as the difference between the global and wrinkling standard deviation (i.e., the gap between blue and red bars in figure 8), increases as the coil charge duration was extended for each operating condition investigated, sometimes in a more evident way when switching from CH10 to CH20 others from CH20 to CH40. Correlating the here findings with the thermodynamic considerations on the COV_{IMEP}, the combustion process stability seems to benefit from the decrease of the wrinkling effect more than the increase of the instability due to flame centre location. Furthermore, in line with the previous seen COV trends, the findings at CA5 seem to suggest that the flame shape plays a more relevant role than its inception location.

Conclusions

The interaction between the early stages of combustion process and combustion instability, as the ignition energy varies, was investigated on an optically accessible DISI engine. The main results achieved with this work are the following:

- The COV_{IMEP}, strongly related with the cycle-to-cycle variability, decreased as the coil charge duration increased, but without having any relevant reflection on the other combustion process parameters. More precisely, it was noted a relative decrease in COV_{IMEP} of about 13% for the WOT operative case and of about 8% for the boosted condition when the coil charge duration was extended from 10 up to 40 CAD.
- The optical investigation revealed an evident increase in arc size and elongation parallel to the grow of spark ignition energy. The analysis on the flame morphology at CA5 and CA10 showed an overall reduction of the wrinkling effect on the flame contour. More in particular, it was observed a relative reduction of the standard deviation (σ) directly linked to the irregularity of the flame edge of about 20 and 15% for the WOT and boosted conditions respectively. Furthermore, despite the average increase in standard deviation relative to the dislocation of flame mass centre, the wrinkling effect was found to be predominant for the combustion stability.

References

[1] https://ec.europa.eu/info/strategy/priorities-2019-2024/european-green-deal/delivering-european-green-deal_en
[2] Reitz RD, Ogawa H, Payri R, et al. IJER editorial: The future of the internal combustion engine. *International Journal of Engine Research*. 2020;21(1):3-10. doi:10.1177/1468087419877990
[3] M.F. M. Sabri, K.A. Danapalasingam, M.F. Rahmat, A review on hybrid electric vehicles architecture and energy management strategies, Renewable and Sustainable Energy Reviews, Volume 53, 2016, Pages 1433-1442, ISSN 1364-0321, https://doi.org/10.1016/j.rser.2015.09.036
[4] hahed, S. M., and Karl-Heinz Bauer. "Parametric Studies of the Impact of Turbocharging on Gasoline Engine Downsizing." *SAE International Journal of Engines*, vol. 2, no. 1, 2009, pp. 1347–58, http://www.jstor.org/stable/26308474
[5] Haiqiao Wei, Tianyu Zhu, Gequn Shu, Linlin Tan, Yuesen Wang, Gasoline engine exhaust gas recirculation – A review, Applied Energy, Volume 99, 2012, Pages 534-544, ISSN 0306-2619, https://doi.org/10.1016/j.apenergy.2012.05.011
[6] Yangyang Li, Xiongbo Duan, Yiqun Liu, Jingping Liu, Genmiao Guo, Yonghao Tang, Experimental investigation the impacts of injection strategies coupled with gasoline/ethanol blend on combustion, performance and emissions characteristics of a GDI spark-ignition engine, Fuel, Volume 256, 2019, 115910, ISSN 0016-2361, https://doi.org/10.1016/j.fuel.2019.115910
[7] https://cordis.europa.eu/project/id/101006841/it
[8] Cecile P., Vincent K., Julien R., Influence of flow and ignition fluctuations on cycle-to-cycle variations in early flame kernel growth, Proceedings of the Combustion Institute, Volume 35, Issue 3, 2015, Pages 2897-2905, ISSN 1540-7489, https://doi.org/10.1016/j.proci.2014.07.037
[9] P.G. Aleiferis, Y. Hardalupas, A.M.K.P. Taylor, K. Ishii, Y. Urata, Flame chemiluminescence studies of cyclic combustion variations and air-to-fuel ratio of the reacting mixture in a lean-burn stratified-charge spark-ignition engine, Combustion and Flame, Volume 136, Issues 1–2, 2004, Pages 72-90, ISSN 0010-2180, https://doi.org/10.1016/j.combustflame.2003.09.004
[10] Xiongbo Duan, Jingping Liu, Zhipeng Yuan, Genmiao Guo, Qi Liu, Qijun Tang, Banglin Deng, Jinhuan Guan, Experimental investigation of the effects of injection strategies on cycle-to-cycle variations of a DISI engine fueled with ethanol and gasoline blend, Energy, Volume

165, Part B, 2018, Pages 455-470, ISSN 0360-5442, https://doi.org/10.1016/j.energy.2018.09.170

[11] Costa, Michela, et al. *Image processing for early flame characterization and initialization of flamelet models of combustion in a gdi engine*. No. 2015-24-2405. SAE Technical Paper, 2015.

Acknowledgments

Authors wishing to acknowledge assistance or encouragement from colleagues, special work by technical staff or financial support from organizations should do so in an unnumbered Acknowledgments section immediately following the last numbered section of the paper.